The Continuous-Flow Gravity Thickener: Steady State Behavior

The equations governing consolidation in a continuous-flow gravity thickener are developed based on the assumption that a flocculated suspension possesses a compressive yield stress $P_y(\phi)$ that is a function of local volume fraction only. These equations are used to model the steady state operation of a thickener. The bed height required to achieve a given underflow concentration is found to be a relatively sensitive function of the details of the $P_y(\phi)$ function, particle flux through the thickener, and variations in the cross-sectional area of the thickener. The limiting values of the underflow concentration ϕ_u for a given flux or the limiting values of flux for a desired ϕ_u are studied and shown to exist only for cylindrical and converging thickeners.

K. A. Landman, L. R. White
Department of Mathematics
University of Melbourne
Parkville, Victoria 3052 Australia

Richard Buscall
Corporate Colloid Science Group
Imperial Chemical Industries PLC
Runcorn, Cheshire WA7 4QE, England

Introduction

In a previous paper (Buscall and White, 1987) we discussed the rheological properties of concentrated suspensions that determine their behavior in consolidation processes of commercial importance such as batch settling, continuous gravity thickening and filtration. In that paper we applied those rheological concepts to batch settling, that is, sedimentation in a closed-bottom container, and demonstrated how laboratory experiments of this type in a centrifuge can be used to determine experimentally the relevant rheological parameters for a particular system. In the present paper we extend this analysis to the steady state operation of a continuous-flow gravity thickener.

In practice, gravity thickeners are not of constant cross section. This may be a deliberate design feature of the vessel to permit a central underflow takeoff or a natural and (unless raked) unavoidable consequence of the buildup of compacted immobile suspension in the bottom corners of the vessel. This buildup can extend to a considerable height in the thickener due to the existence of a shear yield stress that is a rapidly increasing function of particle volume fraction in the flocculated suspension. Such natural funneling structures may be a major cause of underperformance in gravity thickeners of this type. The effect of variable cross section on thickener performance is an important practical problem. The present paper differs from the previous analysis by Dixon (1980) in four important ways:

1. The rheological behavior of the suspension is more accurately modeled.
2. The assumption of plug flow is not made, although our simpler and perhaps more plausible assumption that ϕ does not vary much over a horizontal cross section leads to similar equations.
3. The model trends are compactly summarized in the behavior of a single dimensionless parameter L, which represents a scaled consolidation bed height.
4. The fundamental differences in the behavior of converging and diverging and cylindrical thickeners are discussed for the first time.

Rheology of Consolidation

The first rheological property of significance in settling phenomena is the hydrodynamic resistance of the suspension to flow of the suspending fluid. If v is the local average particle velocity and w is the local average suspending fluid velocity (relative to a laboratory fixed-axes system), then the hydrodynamic drag force F_h per unit volume of suspension that the fluid exerts on the particles at local volume fraction ϕ can be written as

$$F_h = \frac{-\Delta\rho g \phi r(\phi)}{u_{St}} (v - w) \tag{1}$$

where

$$u_{St} = \frac{\Delta\rho g V_p}{\lambda_{St} \eta a_p} \tag{2}$$

is the Stokes settling velocity of an isolated floc—the dilute set-

Correspondence concerning this paper should be addressed to K. A. Landman.

tling velocity limit. The function $r(\phi)$ is the hindered settling factor with the properties

$$r(\phi) \xrightarrow[\phi \to 0]{} 1 \tag{3}$$

$$r(\phi) \xrightarrow[\phi \to 1]{} \infty \tag{4}$$

and is introduced to account for hydrodynamic interactions between the particles. Batchelor (1972) has calculated $r(\phi)$ to first order in ϕ and experimental measurements (Buscall et al., 1982; Kops-Werkhoven and Fijnant, 1982) on spherical particles have established the empirical relationship

$$r(\phi) = (1 - \phi)^{-4.5} \tag{5}$$

An alternate way of expressing $\boldsymbol{F}_h$ is to regard the flow of fluid past the particles in the suspension as equivalent to flow in a porous medium and to connect flow to drag force via the Darcy law relationship

$$v - w = -K(\phi)\boldsymbol{F}_h \tag{6}$$

Clearly the two approaches are equivalent in practice since the hydraulic conductivity can be taken to be defined by Eqs. 1 and 6 as

$$K(\phi) = \frac{u_{St}}{\Delta\rho g \phi r(\phi)} \tag{7}$$

In the present paper, we prefer to use the hindered-drag concept in expressing $\boldsymbol{F}_h$ since as a concept it spans the entire volume fraction range and is not limited to high ϕ. The point is academic since we will regard $r(\phi)$ [or $K(\phi)$] as an experimentally determined quantity, as discussed in Buscall and White (1987). We are not proposing to use the concept to obtain $r(\phi)$ theoretically for a given system. Equation 1 has the further advantage of providing an appropriate scaling of the hydrodynamic drag force that we shall use below.

Aside from hydrodynamic interactions, it must be recognized that the particles of the suspension interact directly with one another and thus give rise to a local particle pressure p. In the absence of any other forces, the particles have size and shape and are in Brownian motion. The resultant particle-particle collisions would be sufficient to establish such a pressure. In addition, in a stable suspension there exist relatively short-range repulsive interactions of electrostatic origin that also contribute to the particle pressure. In such a system, the total particle pressure p can be shown to be thermodynamically equivalent to the osmotic pressure of the particles $P_{os}(\phi)$. That is, at a point in the suspension where the local volume fraction is ϕ, the particle pressure is given by

$$p = P_{os}(\phi) \tag{8}$$

and is thus a function of local volume fraction alone. In high-concentration electrolyte conditions usually pertaining to industrial consolidation $P_{os}(\phi)$ is very small compared to gravitational potential energy changes except as ϕ approaches close packing. Thus, in such stable suspensions the particle pressure p has very little effect on the settling process except in the consolidated bed at the bottom. Because of the short-range nature of the interparticle forces, we really do not need to know much detail about $P_{os}(\phi)$ in the bed. The system can be more or less completely described with the single parameter ϕ_{cp}, the volume fraction at close packing. Because $P_{os}(\phi)$ changes sharply with ϕ for ϕ near ϕ_{cp}, the consolidated bed can be considered to be everywhere at $\phi = \phi_{cp}$ with negligible error. Only at very low electrolyte concentrations where electrostatic forces have ranges comparable to interparticle spacings can $P_{os}(\phi)$ become sufficiently large to influence sedimentation behavior outside the consolidated bed region.

Of far greater importance industrially are the flocculated suspensions for which the above considerations in determining p are inappropriate. It will usually be the case that either electrolyte or polymer flocculants have been added to the suspension with the aim of producing connected aggregate structures of many particles held together by van der Waals or polymer-bridging forces. These flocs have a larger weight to size ratio, Eq. 2, and therefore possess higher settling velocities than the individual particles. Although speeding up the sedimentation rate, the process of flocculation has a second effect on the system. When the individual flocs hit the consolidated bed, the attractive forces between particles due to the bridging flocculant cause the floc to stick to the bed in the position of first contact. The floc is not free to roll around the top of the bed seeking a lower gravitational potential energy. Center of mass Brownian motion of the floc is greatly reduced. Subsequent collisions of other flocs will tend to create an open network of flocculated particles at average volume fraction much lower than can be achieved by a stable sedimenting suspension that is free to seek its lowest gravitational energy configuration.

Once the average particle volume fraction is high enough that a network of connected particles is formed throughout the volume, the suspension takes on the properties of a solid (albeit flimsy) structure. In particular, compressive stresses on the suspension can be transmitted via the network throughout the system and the structure then possesses the ability to support itself. In a flocculated system above this volume fraction the particle pressure p should be more properly thought of as a network pressure.

When such a network has formed throughout the system, we are free to increase p by applying some sort of external compression to the network—for example, push on it with a piston permeable to the suspending fluid or increase the gravitational forces as in a centrifuge. As this process is applied, the network structure will resist further compression and p will increase until the compressive forces become so strong that the structure begins to deform irreversibly. Bonds between particles will rupture, the system will consolidate and, consequently, new and more bonds will form until the network has become strong enough to oppose the compression once more. In flocculated systems we therefore need to invoke a second rheological parameter to properly describe their behavior in consolidation processes. The compressive yield stress $P_y(\phi)$ is defined as the value of the network (particle) pressure at which a flocculated suspension at volume fraction ϕ will no longer resist compression elastically and will start to yield (i.e., irreversibly consolidate).

The compressive yield stress $P_y(\phi)$ is an implicit function of the strength of the interparticle bridging forces and (probably) the previous shear history of the system, which will determine

primary floc size and internal structure. In Buscall and White (1987), we show how equilibrium bed-height measurements in a centrifuge can be used to measure $P_y(\phi)$. The general form of $P_y(\phi)$ for real systems is shown schematically in Figure 1. The main features are the rapidly increasing nature of the function as ϕ increases and the existence of a point ϕ_g (gel point) below which $P_y(\phi)$ cannot be experimentally distinguished from zero. This point may be considered to be the lowest volume fraction at which all the primary flocs are interconnected throughout the container. This critical volume fraction depends strongly on the nature of the flocs, which in turn depends on particle size and shape, type and method of flocculation, and shear history. For spherical particles it can vary between 0.05 and 0.3, depending on particle size (Buscall et al., 1987), and can be as low as 0.01 for highly anisotropic particles.

If we are discussing a networked structure at $\phi_o > \phi_g$ we must distinguish between a structure that is formed by aggregation of fundamental flocs created at a volume fraction less than ϕ_g and that which is formed by flocculation at the given volume fraction ϕ_o. These structures will in general have a different network arrangement and consequently different $P_y(\phi)$ behavior. In the latter case $\phi_g = \phi_o$, the volume fraction at which the network is created.

Power law curves of the type

$$P_y(\phi) = c[(\phi/\phi_g) - 1]^m \tag{9}$$

or

$$P_y(\phi) = c[(\phi/\phi_g)^n - 1] \tag{10}$$

with m varying between 4 and 10 and n varying between 8 and 10 have been fitted to experimental systems such as polystyrene latex (Buscall et al., 1987) and red mud suspensions (De Guingand, 1986). As yet no definitive theory for $P_y(\phi)$ has been constructed, so the physical significance of the fitting parameters c, $m(n)$ (in relation to the network structure and interparticle bond strengths) remains uncertain. However, we note that recently Brown (1987) has analyzed a space-filling system of fractal aggregates and confirmed that a power law relationship exists.

There is a third rheological parameter of paramount importance in the consolidation process in a flocculated, networked system. We have already introduced the concept that when the network pressure exceeds $P_y(\phi)$ at a point in the suspension where the volume fraction is ϕ, the system will locally collapse to form a denser (stronger) structure. To completely describe this process, we must know the kinetics of the collapse process. Dixon (1978) recognized the importance of a kinetic description of collapse in removing certain anomalies in the theory of sedimentation/consolidation that occur if the collapse kinetics are neglected. Independently, we evolved a very similar argument (Buscall and White, 1987). We proposed a general kinetic scheme of the type

$$\frac{D\phi}{Dt} = 0 \qquad p < P_y(\phi) \tag{11}$$

$$= \kappa(\phi, p)[p - P_y(\phi)] \qquad p \geq P_y(\phi) \tag{12}$$

(Here D/Dt is the material derivative. It is needed for following a volume element of flocs that have pressure p.) In Buscall and White (1987) it was reasoned that if p was not too far from $P_y(\phi)$ we could make a simpler assumption:

$$\kappa(\phi, p) = \kappa(\phi) \tag{13}$$

We termed $\kappa(\phi)$ the dynamic compressibility of the suspension. It was argued that if the dynamics of collapse were rate-determined by drainage of the suspending fluid from between the particles as the network consolidated, then $\kappa(\phi)$ could be estimated as

$$\kappa(\phi) \sim \frac{9\phi\left[1 - \left(\frac{6\phi}{\pi}\right)^{1/3}\right]^2}{\eta(1 - \phi)} \tag{14}$$

As discussed in Buscall and White (1987) and later below, Eq. 14 implies that drainage of excess suspending fluid is relatively a very rapid process. We should note, however, that consolidation when $p > P_y(\phi)$ need not be rapid, since collapse may be rate-determined by the breaking and/or reformation of interparticle bonds, which may be considerably slower than the drainage process. No experimental evidence exists for this conjecture and, indeed, preliminary experiments on initial sedimentation rate in flocculated suspensions are not supportive (Buscall and White, 1987). These experiments are in agreement with an initial rate equation calculated on the assumption that collapse is a very rapid process (on the time scale of sedimentation) when the yield stress is exceeded.

We shall assume in this paper that Eqs. 11–13 hold, and further, that $\kappa(\phi)$ is "large" regardless of which step is rate-determining in the collapse process. It follows immediately from Eq. 12 and the assumed magnitude of the dynamic compressibility κ that

$$p \simeq P_y(\phi) \tag{15}$$

(almost) everywhere in the collapsing part of the sediment. Physically, when p exceeds $P_y(\phi)$, collapse is assumed so rapid that, locally, ϕ moves immediately to the value at which $P_y(\phi)$ exactly balances the applied network pressure. Network pressure can, then, never greatly exceed the yield stress in a rapidly

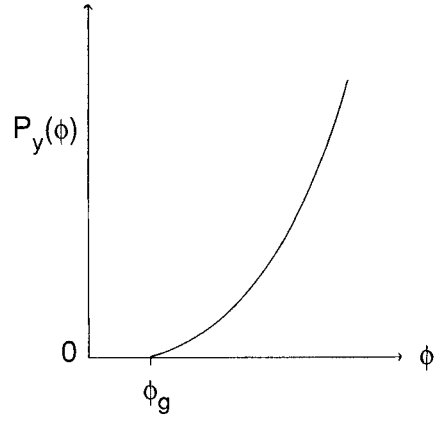

Figure 1. Plot of compressive yield stress $P_y(\phi)$ for real flocculated systems.

collapsing structure. To what extent p can exceed $P_y(\phi)$ we will examine below.

Equation 15 is not new. Several authors (Dixon, 1978, 1980; Tiller and Khatib, 1984; Tiller and Leu, 1980) have made use of a constitutive equation connecting network stress to local volume fraction. As discussed above, stable suspensions obey a constitutive equation (i.e., Eq. 8) since the network pressure is just the osmotic pressure of the particles—which, thermodynamically, is a function of ϕ only. It should be understood, however, that the existence of a constitutive relationship for flocculated suspensions is predicated on the assumption of rapid collapse when yield stress is exceeded.

The above discussion has stressed the importance of three rheological parameters—hindered settling factor $r(\phi)$, compressive yield stress $P_y(\phi)$, and dynamic compressibility $\kappa(\phi)$—in determining sedimentation/consolidation behavior in flocculated systems. When $\kappa(\phi)$ is sufficiently large, we need to know $r(\phi)$ and $P_y(\phi)$ only in order to model the process. Knowledge of the precise magnitude of $\kappa(\phi)$ is important only in a small boundary layer at the top of the consolidating zone and, as we demonstrate below, this region can be neglected in practice.

Sedimentation-Consolidation Equations

Local equations

A balance of forces on the particles in a volume element of the suspension yields

$$-\frac{\Delta\rho g\phi r(\phi)}{u_{St}}(v-w)-\nabla p+\Delta\rho g\phi z=0 \tag{16}$$

As discussed above, the first term in Eq. 16 is the hydrodynamic drag exerted by the suspending fluid on the sedimenting particles. The second term is the net force that the surrounding particles exert by direct interaction on the particles of the volume element. The third term is the net gravitational force exerted on the particles (i.e., weight minus upthrust of suspending fluid). The positive z axis is taken as the direction of gravitational acceleration. We have neglected in this force balance equation the forces exerted by container walls on the neighboring suspension. There will, of course, be a boundary layer of essentially immobile suspension on the side walls over which the rest of the suspension will slip. The viscoelastic properties of the suspension under shear will determine the details of this layer and the transition to bulk suspension behavior. We have also neglected these shear forces in the bulk of the suspension on the grounds that:

1. The system is (it is hoped) close to plug flow where suspension viscosity is unimportant except in the wall boundary layer
2. Experimental measurements (Buscall et al., 1982) of shear yield stresses in flocculated systems reveal that shear yield stresses are several orders of magnitude smaller than compressional yield stresses

Conservation of particle and fluid masses requires the continuity equations

$$\frac{\partial\phi}{\partial t}+\nabla\cdot(\phi v)=0 \tag{17}$$

$$\frac{\partial(1-\phi)}{\partial t}+\nabla\cdot[(1-\phi)w]=0 \tag{18}$$

to hold locally. The final local equations are the kinetic equations, Eqs. 11 and 12, developed above. The material derivative is given by

$$\frac{D\phi}{Dt}=\frac{\partial\phi}{\partial t}+v\cdot\nabla\phi \tag{19}$$

$$=-\phi\nabla\cdot v \tag{20}$$

from Eq. 17. It follows that the kinetic equations reduce to

$$\nabla\cdot v=0 \qquad p<P_y(\phi) \tag{21}$$

$$=\frac{-\kappa(\phi)}{\phi}[p-P_y(\phi)] \qquad p\geq P_y(\phi) \tag{22}$$

that is, the collapse equations contain velocity gradient information.

Cross-sectionally averaged equations

In modeling a gravity thickener most studies assume plug flow, that is, that v, w, ϕ, p are functions of vertical coordinate z alone. In a real thickener these quantities are functions of horizontal position as measured by a radial coordinate x, Figure 2. It is possible to make less restrictive assumptions on v, w, ϕ, p without unnecessarily complicating the analysis.

We take $R(z)$ to be the radius of the thickener measured horizontally from the axis of symmetry of the thickener and

$$A(z)=\pi R^2(z) \tag{23}$$

as the corresponding cross-sectional area at depth z in the bed. For any function $F(z, x, t)$ with position (z, x) we define a corre-

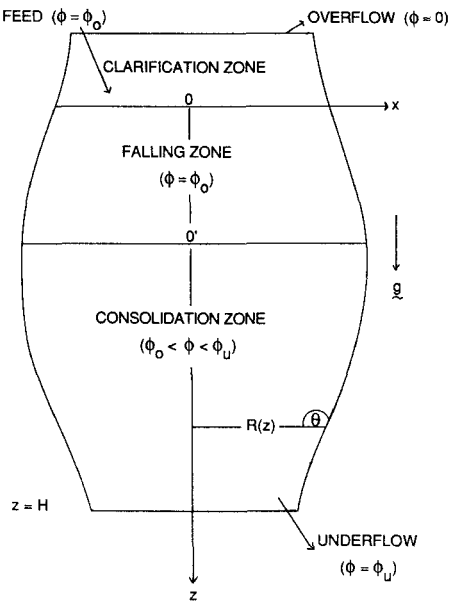

Figure 2. Geometry of a continuous-flow, variable cross section gravity thickener.
If $\phi_o<\phi_g$, origin is at 0', otherwise at 0
Thickener bottom (underflow takeoff point) is at $z=H$

sponding cross-sectionally averaged quantity $\bar{F}(z, t)$ by

$$\bar{F}(z, t) = \frac{1}{A(z)} \int_{A(z)} d^{(2)}\mathbf{x} F(z, \mathbf{x}, t) \tag{24}$$

We note the identity

$$\frac{\partial}{\partial z}[A(z)\bar{F}(z, t)] = A(z)\overline{\frac{\partial F}{\partial z}} + \frac{dA}{dz} F(z, \mathbf{x}, t)|_{|x|=R(z)} \tag{25}$$

which follows from Eq. 24 by differentiation with respect to z.

Cross-sectionally averaging Eq. 17 gives

$$\frac{\partial \bar{\phi}}{\partial t} + \frac{1}{A(z)} \int_{A(z)} d^2\mathbf{x} \nabla \cdot (\phi \mathbf{v}) = 0 \tag{26}$$

Application of the divergence theorem to this equation yields

$$\frac{\partial \bar{\phi}}{\partial t} + \frac{\overline{\partial(\phi v_z)}}{\partial z} + \frac{2\pi R(z)}{A(z)} (\phi v_x)|_{|x|=R(z)} = 0 \tag{27}$$

We impose the kinematic constraint at the thickener wall that the particle velocity must be along the wall, that is,

$$\left(\frac{v_x}{v_z}\right)\Bigg|_{|x|=R(z)} = \frac{dR}{dz} \tag{28}$$

Substitution of this boundary condition into Eq. 27 with the general result, Eq. 25, gives

$$A(z)\frac{\partial \bar{\phi}}{\partial t} + \frac{\partial}{\partial z}[A(z)\overline{\phi v_z}] = 0 \tag{29}$$

A similar argument for fluid conservation Eq. 18 yields

$$A(z)\frac{\partial(1 - \bar{\phi})}{\partial t} + \frac{\partial}{\partial z}[A(z)\overline{(1 - \phi)w_z}] = 0 \tag{30}$$

In steady state operation all functions are independent of time so that these equations reduce to

$$\frac{d}{dz}[A(z)\overline{\phi v_z}] = 0 \tag{31}$$

$$\frac{d}{dz}[A(z)\overline{(1 - \phi)w_z}] = 0 \tag{32}$$

which can be integrated to yield

$$A(z)\overline{\phi v_z} = Q_p \tag{33}$$

and

$$A(z)\overline{(1 - \phi)w_z} = Q_w \tag{34}$$

Here Q_p is the total particle volumetric flow rate and Q_w is the total fluid volumetric flow rate through the thickener at the underflow point.

To proceed, we make the approximation that $\phi(z, x)$ does not vary appreciably over a cross section, that is,

$$\phi(z, \mathbf{x}) \simeq \phi(z) = \bar{\phi}(z) \tag{35}$$

from which it follows that

$$\overline{f(\phi)F(z, \mathbf{x})} = f(\phi)\bar{F}(z) \tag{36}$$

In this approximation, we have

$$\overline{\phi v_z} = \phi(z)\bar{v}_z, \quad \overline{\phi w_z} = \phi(z)\bar{w}_z \tag{37}$$

so that Eqs. 33 and 34 become, respectively,

$$\bar{v}_z = \frac{1}{\phi(z)}\left(\frac{Q_p}{A(z)}\right) \tag{38}$$

$$\bar{w}_z = \frac{1}{1 - \phi(z)}\left(\frac{Q_w}{A(z)}\right) \tag{39}$$

If we assume as a boundary condition at the bottom of the thickener that the average velocities of the particles and fluid are equal, then Eqs. 38 and 39 yield

$$Q_w = \left(\frac{1 - \phi_u}{\phi_u}\right) Q_p \tag{40}$$

Physically, we should not expect significant velocity differences between particles and suspending fluid in the horizontal direction (as opposed to the vertical components) as both particles and fluid move together horizontally as required to follow cross-sectional area variations. Thus, at all stages we will impose on physical grounds

$$v_x = w_x \tag{41}$$

This implies, from Eq. 16, that p has no horizontal variation and in this approximation,

$$p(z, \mathbf{x}) \simeq p(z) = \bar{p}(z) \tag{42}$$

In the consolidation zone this will be entirely consistent with our later approximation, Eq. 15 together with Eq. 35.

Cross-sectionally averaging the vertical component of Eq. 16, we obtain (using Eqs. 35, 37, and 42)

$$-\frac{\Delta\rho g \phi r(\phi)}{u_{St}}(\bar{v}_z - \bar{w}_z) - \frac{dp}{dz} + \Delta\rho g \phi = 0 \tag{43}$$

which can be written with the aid of Eqs. 38–40 as

$$\frac{dp}{dz} = \Delta\rho g \phi \left[1 - \frac{r(\phi)Q_p(1 - \phi/\phi_u)}{u_{St}A(z)\phi(1 - \phi)}\right] \tag{44}$$

Finally we must cross-sectionally average the kinetic equations. Assuming again that ϕ and p do not vary appreciably over a cross section (Eqs. 35 and 42), the righthand side of Eq. 22 remains the same. Using Eqs. 24, 25, and 28, the average of the

lefthand side is

$$\frac{1}{A(z)}\frac{\partial}{\partial z}[A(z)\bar{v}_z]$$

For steady state operation this may be rewritten using Eq. 38 as

$$-\frac{Q_p}{A(z)}\frac{1}{\phi^2}\frac{d\phi}{dz}$$

Hence Eqs. 21 and 22 become:

$$\frac{d\phi}{dz} = 0 \qquad p < P_y(\phi) \qquad (45)$$

$$= \frac{\kappa(\phi)\phi}{[Q_p/A(z)]}[p - P_y(\phi)] \qquad p \geq P_y(\phi) \qquad (46)$$

Physically, Eq. 44 relates the particle pressure at z to the net weight of particles above that depth offset by the hydrodynamic drag on those particles. Clearly, we must require the particle pressure to be zero at the top of the sedimenting column (the feed input point), that is,

$$p(0) = 0 \qquad (47)$$

Here we are neglecting osmotic contributions to p since in consolidating flocculated systems these are negligible compared with the compressive yield stress $P_y(\phi)$ which scales p.

To describe the thickener column, we need to distinguish between the two operational modes, $\phi_o < \phi_g$ and $\phi_o > \phi_g$.

$\phi_o < \phi_g$ Mode of Operation

When the feed volume fraction ϕ_o is less than the critical volume fraction ϕ_g at which the system is completely networked, there is no mechanism for the net weight of particles above a given level to be felt at that level. The individual flocs are in free-fall at the top of the thickener column (albeit hindered by hydrodynamic interaction with neighboring flocs). The particle pressure remains at its value at the top of the column, namely $p(z) = 0$. Hence in this region Eq. 44 reduces to

$$0 = 1 - \frac{r(\phi)Q_p(1 - \phi/\phi_u)}{u_{St}A(z)\phi(1 - \phi)} \qquad (48)$$

which is to be solved for $\phi(z)$ subject to the conditions that Q_p is a constant and that $A = A_0$ and $\phi = \phi_o$ at the height of feed input. It follows from these initial conditions that the local particle volumetric flow rate is then determined as

$$Q_p = \frac{u_{St}A_0\phi_o(1 - \phi_o)}{r(\phi_o)(1 - \phi_o/\phi_u)} \qquad (49)$$

Note that Q_p is a function of the underflow concentration ϕ_u. When a thickener is operated in this mode, the operator has no control over the flow rate in steady state. It is solely determined by the hindered settling rate. For a cylindrical thickener, $A(z) = A_0$ and with this value of Q_p Eq. 48 gives $\phi(z) = \phi_o$ in the falling zone. For noncylindrical thickeners, with a specified $A(z)$ and this value of Q_p it is relatively easy to obtain $\phi(z)$ from Eq. 48. With $r(\phi)$ given by Eq. 5 it is straightforward to show that

$$r(\phi)(1 - \phi/\phi_u)/\phi(1 - \phi) \qquad (50)$$

is a monotonically decreasing function of ϕ in the range $0 < \phi < \phi_u$ provided $\phi_u < 0.52$. Provided that ϕ lies in this range, it follows from this observation that Eq. 48 predicts that $\phi(z)$ increases as $A(z)$ decreases and vice versa. This result is a little surprising since there are no local mechanisms for rarefaction or concentration of the particles, but it may be rationalized by the following argument. Converging thickener walls would tend to concentrate particles falling on them from above at the walls. This would lead to an increase in ϕ near the walls while leaving the inner region near the thickener axis at ϕ_o. Thus $\bar{\phi}$ would increase in this case, as the model predicts. Correspondingly, diverging walls would lead to a decrease in ϕ in their neighborhood and a decrease therefore in $\bar{\phi}$. This state of affairs clearly violates our assumption in Eq. 35 and would also require $v_x < w_x$, that is, the particles would need to fall more vertically than $v_x = w_x$ would allow. That this is not permitted in the falling zone for $\phi_o < \phi_g$ where $p = 0$ indicates a weakness in the local particle force balance equation. However, this difficulty is traditionally ignored and we shall also not investigate it further here.

In fact we need very limited information from the falling zone. We know that somewhere in the thickener there is a rapid transition from free-falling individual flocs at $\phi = \phi_o$ ($p = 0$) to a networked structure at $\phi = \phi_g$ ($p = 0$). Below this point, consolidation occurs ($d\phi/dz > 0$). The position of this transition (the top of the consolidating bed) from ϕ_o to ϕ_g is taken as the origin in this case—point 0′ in Figure 2. The present paper has as its goal the prediction of the height H of this point above the bottom of the thickener necessary to achieve a given underflow concentration ϕ_u for a specified input ϕ_o. The height of the falling zone above the top of the consolidating column is immaterial to this calculation. The existence of the falling zone serves only to determine the particle volumetric flow rate Q_p permitted for steady state operation, Eq. 49.

In this mode of operation, the top of the consolidation zone is the point where $d\phi/dz$ becomes positive. Since $\phi = \phi_g$, $P_y(\phi_g) = 0$, and $z = 0$ here, from Eqs. 44–46 we require that

$$1 - \frac{A_0}{A(0)}\left[\frac{r(\phi_g)}{r(\phi_o)}\frac{\phi_o}{\phi_g}\frac{1 - \phi_o}{1 - \phi_g}\frac{1 - \phi_g/\phi_u}{1 - \phi_o/\phi_u}\right] > 0 \qquad (51)$$

The term in square brackets is less than unity; this follows from the discussion of the function in Eq. 50. Therefore this inequality will automatically be satisfied when $A(0) \geq A_0$, that is, for cylindrical and diverging thickeners. For a converging thickener, the origin $z = 0$ should be determined so that $A_0/A(0)$ does not violate the inequality of Eq. 51 for any desired ϕ_u.

When $\phi_o < \phi_g$, we must solve Eqs. 44–46 when Eq. 51 is satisfied, from the top of the bed $z = 0$ where $\phi = \phi_g$ to the underflow point $z = H$ where $\phi = \phi_u$, when Q_p is given by Eq. 49.

$\phi_o > \phi_g$ Mode of Operation

In this mode of operation we assume that ϕ_o has been reached by consolidation rather than that the network has formed immediately at ϕ_o by flocculation. This situation would occur in practice when the feed is the underflow from another thickener. The

input feed is completely networked and the particle net weight is transmitted down the column from the position of input to the thickener bottom via the network. However, consolidation cannot occur until the network pressure p has increased above $P_y(\phi_o)$. The flow rate Q_p is no longer determined by hindered settling considerations but is set by the underflow pumping rate (which equals the feed input rate for steady state operation). In this case we take the feed point as the origin of the bed—point 0 in Figure 2. There will be a region at the top of the column ($0 < z < z_c$) where the volume fraction will be given by

$$p(z) < P_y(\phi) \quad 0 < z < z_c \tag{53}$$

since the network pressure $p(z)$ in this region is not large enough to exceed the yield stress, that is,

$$p(z) < P_y(\phi) \quad 0 < z < z_c \tag{53}$$

Hence Eqs. 44 and 52 give

$$\frac{dp}{dz} = \Delta\rho g\phi_o\left[1 - \frac{r(\phi_o)Q_p(1 - \phi_o/\phi_u)}{u_{St}A(z)\phi_o(1 - \phi_o)}\right] \tag{54}$$

The position z_c, which marks the boundary between the falling zone ($\phi = \phi_o$) and the consolidation zone ($d\phi/dz > 0$, $\phi_o < \phi < \phi_u$), is the point at which the network pressure becomes equal to the compressive yield stress $P_y(\phi_o)$ of the network. Clearly the existence of such a point z_c and a consolidation zone may limit the value of the particle flow rate Q_p. It follows from the above discussion that a necessary condition for the existence of a consolidation region is that

$$1 - \frac{r(\phi_o)Q_p(1 - \phi_o/\phi_u)}{u_{St}A(z_c)\phi_o(1 - \phi_o)} > 0 \tag{55}$$

Below we show that this inequality places limits on Q_p and ϕ_u for certain thickener shapes.

$A(z) \le A_0$ for all values of z

This covers thickeners that are cylindrical or consist of cylindrical and converging sections. Then if the inequality in Eq. 55 holds, we have

$$1 - \frac{r(\phi_o)Q_p(1 - \phi_o/\phi_u)}{u_{St}A_0\phi_o(1 - \phi_o)} > 0 \tag{56}$$

This inequality can be interpreted in two ways. The first interpretation is that if Q_p, A_0, and ϕ_o are given for a thickener, then there exists an upper bound on the value of $\phi_u(>\phi_o)$. Larger values of particle flux Q_p/A_0 mean that less consolidation is possible (ϕ_u will be smaller). The (theoretical) limit that $Q_p/A_0 \to \infty$ means that $\phi_u \to \phi_o^+$. The second interpretation is that if a certain underflow volume fraction ϕ_u is desired from the feed volume fraction ϕ_o, then the flux Q_p/A_0 will have to be set sufficiently small that the condition of Eq. 56 holds.

$A(z)$ increasing function of z

This covers all diverging thickeners. In this case we will show that for given values of Q_p and ϕ_o any desired ϕ_u can be attained, and alternatively, if a certain ϕ_u is desired from a ϕ_o then there is no limit on Q_p provided that a wide or tall enough thickener can be constructed. Therefore there are theoretically no constraints on Q_p and ϕ_u. Clearly if the parameter values are chosen so that Eq. 56 holds, then $dp/dz > 0$ for $0 < z < z_c$ and $d\phi/dz > 0$ for $\phi_o < \phi < \phi_u$, $z_c < z < H$ (and Eq. 55 holds). Hence the desired ϕ_u is attained. For the case when Eq. 56 is violated, it is possible to calculate the smallest z value, denoted by z_d, such that

$$\frac{r(\phi_o)Q_p(1 - \phi_o/\phi_u)}{u_{St}A(z_d)\phi_o(1 - \phi_o)} = 1 \tag{57}$$

Then for $z > z_d$, $A(z) > A(z_d)$ and therefore from Eqs. 54, 45, and 46, $dp/dz > 0$ in the falling zone, [$p(z_d) = 0$], and $d\phi/dz > 0$ in the consolidating zone. Hence the desired ϕ_u is attained for any given Q_p provided $A(z_d)$ satisfies Eq. 57. The above comments imply that $dp/dz < 0$ for $0 < z < z_d$ from Eq. 54, and hence would imply negative values of p. This is not permitted and indicates a weakness in the local particle force balance. This equation is traditionally only assumed to hold for $dp/dz \ge 0$. The physical situation it describes is that the flux $Q_p/A(z)$ is sufficiently large that the whole suspension, composed of fluid and particles, is in free-fall and in that region $\phi = \phi_o$ and $p = 0$.

$A(z) \ge A_0$ for certain values of z

This case consists of thickeners not covered in the first case above; it is more general than the second case in that it covers thickeners that are not diverging for all z. A similar result to that in the second case holds and relies on a region $z_d \le z \le z_c$ where $A(z_d) < A(z)$, where again z_d is given by Eq. 57. This fact implies that the condition in Eq. 55 holds and hence consolidation to the desired ϕ_u is attained.

From the above discussion, we can now solve Eq. 54. In the falling zone $\phi = \phi_o$ and

$$p(z) = \begin{cases} 0 & 0 \le z \le z^* \\ \Delta\rho g\phi_o(z - z^*)\left[1 - \dfrac{r(\phi_o)Q_p(1 - \phi_o/\phi_u)}{u_{St}\phi_o(1 - \phi_o)}\dfrac{1}{(z - z^*)}\right. & \\ \left. \cdot \displaystyle\int_{z^*}^{z}\frac{dz}{A(z)}\right], & z^* < z < z_c. \end{cases} \tag{58}$$

where

$$z^* = \begin{cases} 0 & \text{if Eq. 56 holds} \\ z_d & \text{if Eq. 56 does not hold but Eq. 57 does} \end{cases} \tag{59}$$

The point z_c is defined as $p(z_c) = P_y(\phi_o)$, hence it is determined by

$$P_y(\phi_o) = \Delta\rho g\phi_o(z_c - z^*) \cdot\left[1 - \frac{r(\phi_o)Q_p(1 - \phi_o/\phi_u)}{u_{St}\phi_o(1 - \phi_o)}\frac{1}{(z_c - z^*)}\int_{z^*}^{z_c}\frac{dz}{A(z)}\right] \tag{60}$$

Once z_c is determined the problem is reduced to solving Eqs. 44–46 from $z = z_c$, $\phi = \phi_o$, $p = P_y(\phi_o)$ to $z = H$ where $\phi = \phi_u$. Again we wish to calculate the height H necessary to achieve a specified ϕ_u for given Q_p, ϕ_o, $A(z)$. Clearly, for a consolidation zone to exist we require $z_c < H$; this condition in Eq. 60 gives rise to an

inequality relating Q_p, H, $P_y(\phi_o)$, ϕ_o, and ϕ_u. We note that the particle flux Q_p, in the $\phi_o > \phi_g$ mode of operation, is a parameter set by the operator (unlike the $\phi_o < \phi_g$ mode). We finally remark that if $\phi_o = \phi_g$—that is, the system is first flocculated at volume fraction ϕ_o—the above analysis is valid and $z_c = 0$.

Scaled Steady State Equations

It will prove convenient to introduce the following dimensionless variables:

$$Z = z/H \tag{61}$$

$$\Phi(Z) = \phi(z)/\phi_u \tag{62}$$

$$\Pi(Z) = p(z)/P_y(\phi_u) \tag{63}$$

$$f(\Phi) = P_y(\phi)/P_y(\phi_u) \tag{64}$$

$$B(\Phi, \phi_u, \phi_o) = \frac{\left(\frac{\phi_o}{\phi_u}\right)(1 - \phi_o)r(\phi_u\Phi)(1 - \Phi)}{(1 - \phi_u\Phi)r(\phi_o)\Phi} \tag{65}$$

$$\Lambda(\Phi) = \frac{Q_p/A_0}{HP_y(\phi_u)\kappa(\phi)} \tag{66}$$

$$\beta = \frac{(Q_p/A_0)r(\phi_o)}{u_{St}\phi_o(1 - \phi_o)} \tag{67}$$

$$L = \frac{\Delta\rho g\phi_u H}{P_y(\phi_u)} \tag{68}$$

$$a(Z) = A(z)/A_0 \tag{69}$$

The parameter β can be taken as the scaled flux. Note that

$$\beta = 1/(1 - \phi_o/\phi_u) \tag{70}$$

in the $\phi_o < \phi_g$ mode of operation, from Eq. 49, but is variable (within limits, for cylindrical and converging thickeners) in the $\phi_o > \phi_g$ mode. The dimensionless group L can be regarded as a scaled thickener height.

In these scaled variables, Eqs. 44–46 can be written as

$$\frac{d\Pi}{dZ} = L\Phi\left[1 - \frac{\beta}{a(Z)}B(\Phi, \phi_u, \phi_o)\right] \tag{71}$$

$$\frac{d\Phi}{dZ} = 0 \qquad \Pi < f(\Phi) \tag{72}$$

$$= \frac{\Phi a(Z)}{\Lambda(\Phi)}[\Pi - f(\Phi)] \qquad \Pi \geq f(\Phi) \tag{73}$$

A full description of the steady state cylindrical thickener would necessitate the solution of Eqs. 71–73 from $Z = Z_c$, $\Phi = \Phi_c$ to $Z = 1, \Phi = 1$ where

$$(\Phi_c, Z_c) = (\phi_g/\phi_u, 0) \qquad \phi_o < \phi_g \tag{74}$$

$$= (\phi_o/\phi_u, z_c/H) \qquad \phi_o \geq \phi_g \tag{75}$$

For a consolidation zone to exist in the column for the $\phi_o > \phi_g$ mode we require $Z_c < 1$.

Large Dynamic Compressibility Approximation

To solve Eqs. 71–73 in general, we need to specify $r(\phi)$, $P_y(\phi)$, and $\kappa(\phi)$. As discussed above, $r(\phi)$ and $P_y(\phi)$ can be found experimentally from initial sedimentation rate and equilibrium bed height measurements as functions of g in a closed column of the suspension. The dynamic compressibility $\kappa(\phi)$, when sufficiently large, need not be specified as we shall now demonstrate.

Scaling Eqs. 61, 62 and 69 imply that Φ, $d\Phi/dZ$ and $a(z)$ are order $1 \cdot [\mathcal{O}(1)]$ in the consolidating bed. It follows immediately from Eq. 73 that

$$\Pi = f(\Phi) + \mathcal{O}(\Lambda) \tag{76}$$

or, in unscaled variables,

$$p = P_y(\phi) + P_y(\phi_u)\mathcal{O}(\Lambda) \tag{77}$$

This simple scaling argument is sufficient to show that when the dynamic compressibility is large [i.e., $\Lambda(\Phi) \ll 1$], the local network pressure in the consolidation zone exceeds the local compressive yield stress by an $\mathcal{O}(\Lambda)$ small amount.

If we estimate Q_p/A_0 by $u_{St}\phi_u$ (from Eq. 44) and $P_y(\phi_u)$ by $\Delta\rho g\phi_u H$ and use the viscous drainage estimate, Eq. 14, for $\kappa(\phi)$, we have that

$$\Lambda \sim (a_p/H)^2 \tag{78}$$

where a_p is a typical particle dimension. Thus if viscous drainage is rate-determining in the collapse process, we see, from Eq. 78, that Λ is $\mathcal{O}(10^{-8}$–$10^{-12})$. In this paper we will assume that $\Lambda \ll 1$ and write, therefore,

$$p(z) = P_y[\phi(z)] \tag{79}$$

or

$$\Pi(Z) = f[\Phi(Z)] \tag{80}$$

to an excellent approximation in the consolidation zone. The collapse equation, Eq. 73, is no longer needed in this approximation, and substituting Eq. 80 into Eq. 71 we obtain

$$\frac{d\Phi}{dZ} = \frac{L\Phi}{f'(\Phi)}\left[1 - \frac{\beta}{a(Z)}B(\Phi, \phi_u, \phi_o)\right] \tag{81}$$

The problem is thus reduced to the solution of nonlinear first-order ordinary differential Eq. 81 in the consolidation zone.

As noted by Dixon (1978) there is a region at the boundary between the falling and consolidation zones where Eq. 81 is not strictly valid. To see this, we note that Eq. 81 predicts a nonzero $d\Phi/dZ$ in the limit $Z \to Z_c^+$, whereas the exact Eqs. 71–73 would require $d\Phi/dZ$ to be zero at Z_c [where, by definition, $\Pi = f(\Phi_c)$]. There is obviously a boundary layer in the neighborhood of $Z = Z_c$ where the slope changes from zero to the $Z = Z_c^+$ limit of Eq. 81.

The nature of this boundary layer is analyzed in some detail in the Appendix. There we demonstrate that the solution $\Phi^{(0)}(Z)$ of the [large $\kappa(\phi)$] approximate Eq. 81, which we shall exhibit in the next section, differs from the solution of the exact Eqs. 71–73 by, at most, an amount $-\Lambda_c(d\Phi^{(0)}/dZ)|_{Z_c}/[a(Z_c)\Phi_c f'(\Phi_c)]$.

The region where $(d\Phi^{(0)}/dZ)$ differs from $d\Phi/dZ$ is of thickness $\Lambda_c/[a(Z_c)\Phi_c f'(\Phi_c)] \ll 1$. We therefore can neglect this region for large $\kappa(\phi)$ with negligible error.

Numerical Results

In the numerical calculations outlined below we use the Eq. 10 form for $P_y(\phi)$ so that

$$f(\Phi) = \frac{\Phi^n(\phi_u/\phi_g)^n - 1}{(\phi_u/\phi_g)^n - 1} \tag{82}$$

with $n = 5, 9$. Equation 5 is used for $r(\phi)$.

The most efficient solution of differential Eq. 81 is achieved by rescaling Z to incorporate the dimensionless number L defined by Eq. 68. We define

$$Y = LZ = z\left(\frac{\Delta\rho g\phi_u}{P_y(\phi_u)}\right) \tag{83}$$

and write Eq. 81 as

$$\frac{dY}{d\Phi} = \frac{f'(\Phi)}{\Phi\left[1 - \dfrac{\beta}{\alpha(Y)}B(\Phi, \phi_u, \phi_o)\right]} \tag{84}$$

where

$$\alpha(Y) = a(Z) = A(z)/A_0 \tag{85}$$

The starting value of Y we denote Y_c where

$$Y_c = LZ_c \tag{86}$$

To illustrate the effects of variable cross section we chose straight-sided walls where

$$R(z) = R_0 + (z + z_0)\cot\theta \tag{87}$$

where R_0 is the radius at the feed input point, $-z_0$ is the z coordinate of the feed input position, and θ is the angle the wall makes with the interior horizontal. Clearly the value of z_0 is only required when $\theta \neq 0$ and we then have

$$\begin{aligned} z_0 &= \text{free parameter} \quad &&\text{when origin is at 0', } \phi_o < \phi_g \\ z_0 &= 0 \quad &&\text{when origin is at 0, } \phi_o > \phi_g \end{aligned} \tag{88}$$

(when $\phi_o < \phi_g$, z_0 can be fixed by the thickener operator). Note that $\theta < \pi/2$ implies diverging walls, $\theta = \pi/2$ corresponds to a cylindrical thickener, and $\theta > \pi/2$ implies converging walls. Thus, since $A_0 = \pi R_0^2$, we have

$$\alpha(Y) = [1 + \sigma(Y + Y_0)]^2 \tag{89}$$

where

$$\sigma = \frac{P_y(\phi_u)\cot\theta}{\Delta\rho g\phi_u R_0} \tag{90}$$

and Y_0 is the scaled z_0 coordinate, Eq. 83.

With ϕ_o, ϕ_g, ϕ_u, β, σ specified and $f(\Phi)$ given by Eq. 82, we solve Eq. 84 from $\Phi = \Phi_c$, $Y = Y_c$ to the thickener bottom where $\Phi = 1$ and $Y = L$. In this way we determine the value of L (the scaled thickener bed height) sufficient to achieve the desired underflow concentration ϕ_u for specified ϕ_o, ϕ_g, β, σ. Clearly

$$L = L(\phi_u, \phi_o, \phi_g, n\beta, \sigma) \tag{91}$$

It proves convenient to discuss the numerical results for the $\phi_o > \phi_g$ mode of operation first because it is mathematically a more general case; in the $\phi_o < \phi_g$ mode of operation β is fixed in terms of ϕ_o/ϕ_u by Eq. 70 and is not an independent variable.

In Figures 3–5 we plot the scaled bed height L as a function of the underflow volume fraction ϕ_u in the $\phi_o > \phi_g$ mode of operation for various values of σ and scaled flux β. In these sets of curves $\phi_o = 0.125$ and $\phi_g = 0.1$. For each of the cases Y_c can be determined from Eq. 60 using Eqs. 88 and 89. We find that Y_c is the larger positive zero of the following function:

$$\begin{aligned} g(Y_c) = \sigma Y_c^2 + Y_c[1 - \sigma Y^* &- \frac{\beta(1 - \phi_o/\phi_u)}{1 + \sigma Y^*} - \frac{\sigma\phi_u}{\phi_o}f(\phi_o/\phi_u)] \\ &- [Y^* - \frac{Y^*\beta(1 - \phi_o/\phi_u)}{1 + \sigma Y^*} + \frac{\phi_u}{\phi_o}f(\phi_o/\phi_u)] \end{aligned} \tag{92}$$

where Y^* is the scaled z^* coordinate in Eq. 59. From Eqs. 56,

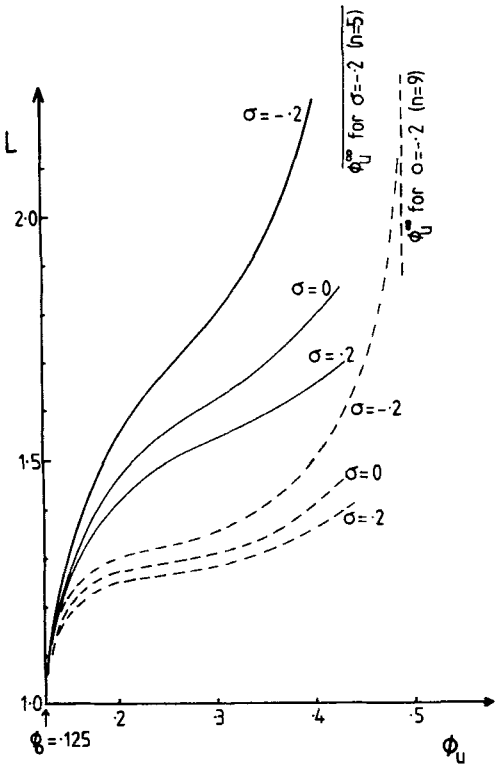

Figure 3. Scaled bed height L vs. underflow concentration ϕ_u for a steady state thickener in $\phi_o > \phi_g$ mode.

$\phi_o = 0.125$, $\phi_g = 0.1$; flux $\beta = 1$; σ = wall slope
Function $f(\Phi)$ chosen per Eq. 82: —— $n = 5$, - - - $n = 9$

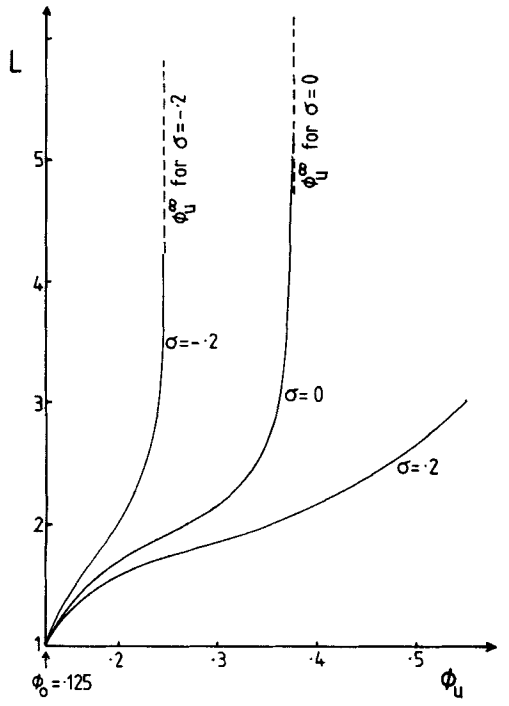

Figure 4. Scaled bed height L vs. underflow concentration ϕ_u for a steady state thickener in $\phi_o > \phi_g$ mode.

$\phi_o = 0.125$, $\phi_g = 0.1$; flux $\beta = 1.5$; σ = wall slope
Function $f(\Phi)$ chosen per Eq. 82 with $n = 5$

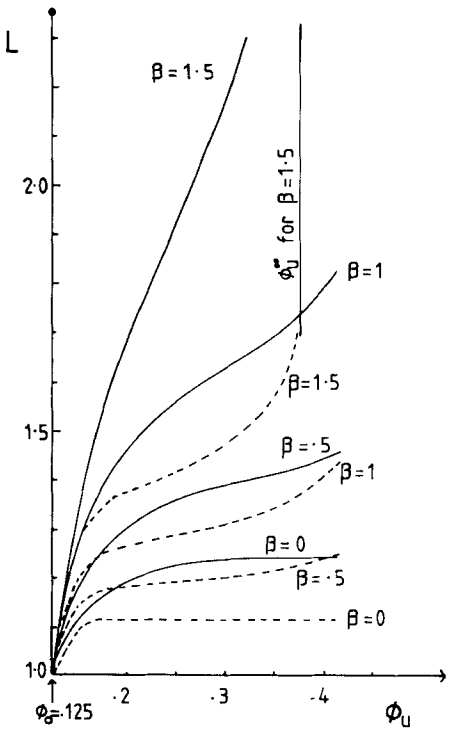

Figure 5. Scaled bed height L vs. underflow concentration ϕ_u for a steady state cylindrical thickener in $\phi_o > \phi_g$ mode.

$\phi_o = 0.125$, $\phi_g = 0.1$; β = flux
Eq. 82: —— $n = 5$, - - - $n = 9$

57, 88, and 89 we have

$$Y^* = \begin{cases} 0 & \beta(1 - \phi_o/\phi_u) < 1 \\ \dfrac{\sqrt{\beta(1 - \phi_o/\phi_u)} - 1}{\sigma} & \sigma > 0,\ \beta(1 - \phi_o/\phi_u) > 1 \end{cases} \tag{93}$$

For a consolidation zone to exist in the thickener, we require $Y_c < L$; hence from Eq. 92, $g(L) > 0$. This inequality involves L, β, σ, ϕ_o, ϕ_u. For all the curves, we note that $L > 1$, (this can be demonstrated analytically by simple inequality arguments on Eq. 44), and $L \to 1$ for $\phi_u \to \phi_o^+$. Note that even when the scaled bed height L only changes by a factor of two over a considerable ϕ_u range, the physical bed height H would vary by a far greater amount since the scaling quantity $P_y(\phi_u)$ is a strongly varying function of ϕ_u. Both $n = 5$ and $n = 9$ forms of $f(\Phi)$ are considered. We note from Figures 3 and 5 that the more compressible the network (which corresponds to larger values of n in Eq. 82) the smaller the bed height required to obtain a given ϕ_u.

The figures clearly illustrate the large variation in the bed height with σ, the slope of the thickener side walls. The bed height increases (decreases) considerably for a converging (diverging) thickener for each desired value of ϕ_u. This behavior was anticipated on physical grounds since the particles fall at a slower velocity in a diverging thickener and thus are able to consolidate to a given ϕ_u in a shorter distance. Further, examination of Eq. 84 shows that $dY/d\Phi$ is smaller (larger) when $\sigma > 0$ ($\sigma < 0$) than when $\sigma = 0$.

Figure 5 and comparison of Figures 3 and 4 for $n = 5$ show that the larger the flux β, the taller the bed for a given ϕ_u and σ.

For comparison, the scaled bed height L in a static cylindrical column of suspension which has $\phi = \phi_u$ at the bottom is also illustrated as the $\beta = 0$ curve in Figure 5; these correspond to zero throughput and give the minimum bed height for each ϕ_u value. In these figures we see that for some values of β and σ there exists a ϕ_u at which the bed height becomes infinite. For a cylindrical thickener ($\sigma = 0$, Figure 5) it is easy to show that this happens for each value of $\beta > 1$. This will occur whenever $dY/d\Phi$ becomes infinite in the solution of Eq. 84, that is, when

$$1 - \beta B(\Phi, \phi_u, \phi_o) = 0 \qquad \sigma = 0 \tag{94}$$

As discussed previously, B is a monotonically decreasing function of Φ in the range $\Phi_c < \Phi < 1$ for $r(\phi)$ given by Eq. 5, provided $\phi_u < 0.52$. Hence for values of ϕ_u smaller than this, it follows that Eq. 94 will be satisfied first at the smallest value of Φ (i.e., Φ_c) in the consolidating bed. From Eq. 65 we see that

$$B(\Phi_c, \phi_u, \phi_o) = 1 - \phi_o/\phi_u \qquad \sigma = 0 \tag{95}$$

so that the bed height will tend to infinity as β tends to the limiting value of

$$\beta^\infty = \frac{1}{1 - \phi_o/\phi_u} > 1 \qquad \sigma = 0 \tag{96}$$

Alternatively, for any given $\beta > 1$ and ϕ_o, the corresponding $L(\phi_u)$ curve will possess a vertical asymptote at

$$\phi_u^\infty = \phi_o\left(\frac{\beta}{\beta - 1}\right) \qquad \sigma = 0 \tag{97}$$

This equation will be independent of the form of $r(\phi)$ provided $r(\phi)$ is such as to make B a monotonically decreasing function of Φ. Also, for a cylinder this asymptote is independent of exponent n in $f(\Phi)$.

Figures 3 and 4 illustrate that for the converging thickener ($\sigma < 0$) there is also an asymptote and it occurs for smaller values of ϕ_u than for the cylindrical thickener. The above argument can be generalized for noncylindrical thickeners. We observe that in this case $dY/d\Phi$ becomes infinite when

$$1 - \frac{\beta B(\Phi, \phi_u, \phi_o)}{\alpha(Y)} = 0 \tag{98}$$

Since B monotonically decreases to zero in the range $\Phi_c \le \Phi \le 1$, ($\phi_u < 0.52$) and when $\alpha(Y)$ decreases for all $Y_c < Y < L$, ($\sigma < 0$), the function on the lefthand side of Eq. 98 will have a minimum for some value of $\Phi < 1$. This minimum will be positive for small values of β and ϕ_u. However, this minimum will become zero (and hence satisfy Eq. 98) for some β^∞ for fixed ϕ_u, or alternatively for some value of ϕ_u^∞ for fixed β. It is not possible to write explicit expressions for β^∞ and ϕ_u^∞ for this noncylindrical case. We see in Figure 3 that the converging thickener exhibits this limiting behavior when $\beta = 1$ (whereas the cylindrical thickener only does for $\beta > 1$) and it is clearly a function of exponent n in $f(\Phi)$. This is due to the Y dependence in Eq. 98 and the n dependence in the definition of Y_c. In Figure 4 the limits on ϕ_u are shown for $\beta = 1.5$ and $n = 5$. [One cannot strictly call it an asymptote since $\alpha(L) = (1 + \sigma L)^2 > 0$. Thus there is a natural cutoff for L at $L = -1/\sigma = 5$ here.] For the other case when $\alpha(Y)$ is an increasing function ($\sigma > 0$), B and $1/\alpha$ are monotonically decreasing functions of Φ and Y, respectively, and therefore B/α has its minimum value at $\Phi = \Phi_c$, $Y = Y_c$. However, we showed in a previous discussion for diverging thickeners that

$$1 - \frac{\beta B(\Phi_c, \phi_u, \phi_o)}{\alpha(Y_c)} > 0 \tag{99}$$

Hence no asymptote exists for diverging thickeners. This fundamental difference in the behavior of variable cross section thickeners is clearly illustrated in Figure 4 for $\beta = 1.5$.

The $\phi_o < \phi_g$ mode of operation is illustrated in Figures 6–8. The flocculated suspension is chosen to have $\phi_g = 0.1$. In Figure 6 we display the concentration profile in a steady state cylindrical thickener ($\sigma = 0$) operating to produce $\phi_u = 0.3$ underflow. The results for two forms of $f(\Phi)$ are shown; the continuous curves are for $n = 5$ and the dashed curves are for $n = 9$. The vertical sections of each graph indicate the hindered settling zone where $\phi = \phi_o$. The horizontal section marks the beginning of the consolidation zone where the volume fraction jumps from ϕ_o to ϕ_g. The limiting behavior in a thickener as the feed concentration ϕ_o is reduced to zero has been illustrated. As ϕ_o increases we see that the bed height must increase in order to maintain $\phi_u = 0.3$. This is due to the fact that as ϕ_o increases, the drag on the falling suspension increases [through the $r(\phi)$ factor] and the effective weight of the network particles—and hence the network pressure gradient—is correspondingly reduced. The bed must therefore be taller in order that the network pressure achieves $P_y(\phi_u)$ at the underflow position. For the parameters used here, as $\phi_o \to \phi_g^-$ the drag force tends to exactly balance the particle weight and $dp/dY \to 0$. In this limit, infinite bed height is required to achieve $\phi_u = 0.3$. Again note that the $n = 9$ profiles show that less bed height is required to obtain $\phi_u = 0.3$ than in the $n = 5$ profiles.

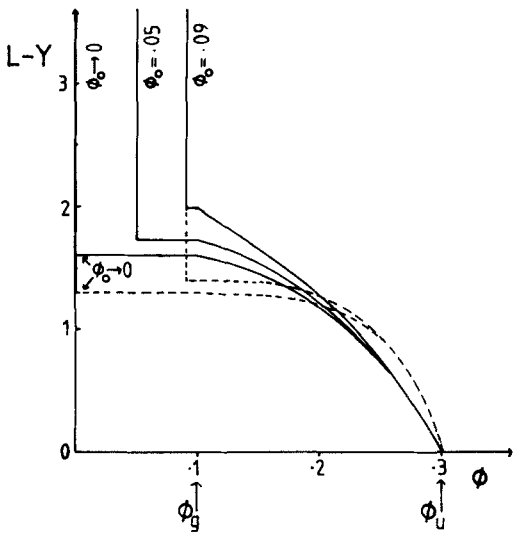

Figure 6. Concentration profiles in a steady state cylindrical thickener producing $\phi_u = 0.3$ underflow in $\phi_o < \phi_g$ mode.

$\phi_g = 0.1$; ϕ_o = feed concentration
Function $f(\Phi)$ chosen per Eq. 82: —— $n = 5$, - - - $n = 9$

In Figures 7 and 8 we plot the scaled bed height L required to achieve a given underflow volume fraction ϕ_u for various ϕ_o values ($\phi_o < \phi_g = 0.1$). For the $\sigma \neq 0$ cases we have set $Y_0 = 0$, defined in Eq. 88. It can be shown that for converging thickeners ($\sigma < 0$), the bed height L increases as Y_0 increases (since $dY/d\Phi$ increases), hence the total height from the feed point to underflow point, $L + Y_0$, increases with Y_0. For diverging thickeners,

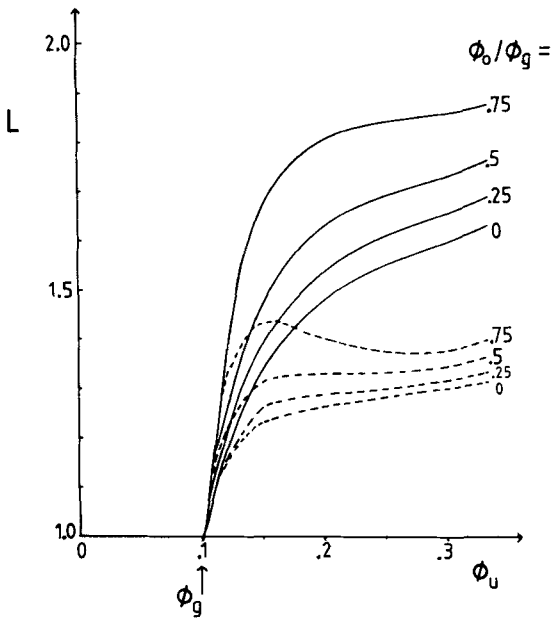

Figure 7. Scaled bed height L vs. underflow concentration ϕ_u for a steady state cylindrical thickener in $\phi_o < \phi_g$ mode.

$\phi_g = 0.1$; Eq. 82: —— $n = 5$, - - - $n = 9$

the bed height L decreases as Y_0 increases (since $dY/d\Phi$ decreases) but the total height from the feed point, $L + Y_0$, increases as Y_0 increases (we checked this numerically for various Y_0 values). Hence setting $Y_0 = 0$ for a noncylindrical thickener gives a lower bound of the total height of the feed point to the underflow point. On each curve the scaled flux β is a function of ϕ_u from Eq. 70. For all curves we again note that $L \geq 1$ for $\phi_u \geq \phi_g$. The case $\phi_o/\phi_g = 0$ is unphysical but gives a lower bound for L for each fixed σ and ϕ_o ($<\phi_g$). As ϕ_o increases, L increases in order to maintain any given ϕ_u, since the flux β increases through Eq. 70.

Figure 8, as with the other mode of operation, illustrates how the bed height increases (decreases) considerably for a converging (diverging) thickener. Further, only converging thickeners exhibit a limiting value of ϕ_u, called ϕ_u^∞. By the same argument as used in the $\phi_o > \phi_g$ mode, with $\beta = 1/(1 - \phi_o/\phi_u)$ and when $\alpha(Y) \geq 1$, the function

$$1 - \frac{B(\Phi, \phi_u, \phi_o)}{\alpha(Y)(1 - \phi_o/\phi_u)}$$

monotonically increases for $(\phi_g/\phi_u) = \Phi_c < \Phi < 1$, $0 \leq Y \leq L$. Its maximum value occurs at Φ_c and is positive for each $\phi_o < \phi_g$. Hence $dY/d\Phi$ is never infinite and there is no limiting value of ϕ_u for cylindrical and diverging thickeners. Clearly when $\alpha(Y)$ is a decreasing function, the function above can become zero at some Φ and Y (by the same argument as in the other operational mode) and hence a ϕ_u^∞ exists for converging thickeners.

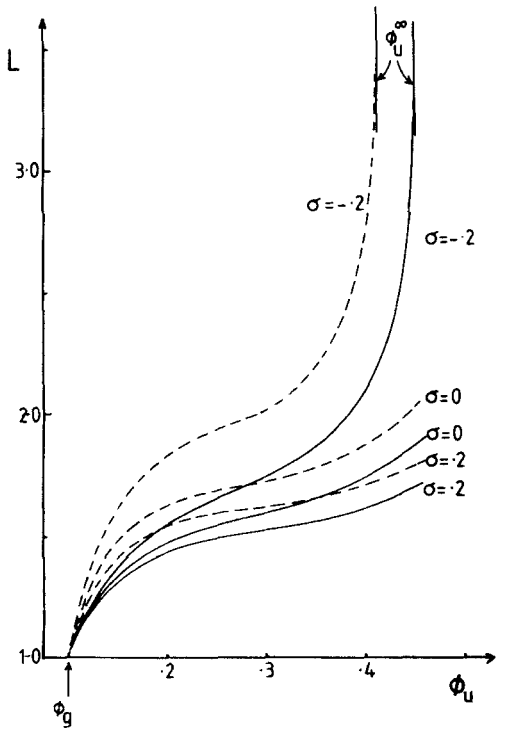

Figure 8. Scaled bed height L vs. underflow concentration ϕ_u for a steady state thickener in $\phi_o < \phi_g$ mode.

$\phi_g = 0.1$; —— $\phi_o/\phi_g = 0$, – – – $\phi_o/\phi_g = 0.5$
Function $f(\Phi)$ chosen per Eq. 82 with $n = 5$; Y_0, Eq. 89, chosen to be zero

Conclusions

The modeling of the consolidation process in a continuous-flow gravity thickener as outlined herein can be of direct value in designing a thickener for a particular suspension. Our results indicate that the bed height is a quite sensitive function of the compressive yield $P_y(\phi)$ curve, the particle flux, and variations in the cross-sectional area of the thickener. The experimental evaluation of $P_y(\phi)$ and $r(\phi)$ for the suspension as discussed in Buscall and White (1987) are of paramount importance.

We have shown quantitatively how the bed height increases (decreases) for a converging (diverging) thickener for each desired value of underflow volume fraction ϕ_u. Also, for sufficiently large values of the flux, when $\phi_o > \phi_g$ there is an upper limit to the ϕ_u that can be attained for converging and cylindrical thickeners but not for diverging ones. Similarly when $\phi_o < \phi_g$ there is an upper limit to ϕ_u for converging thickeners. Hence diverging thickeners have the advantage that any desired ϕ_u can be attained (for any flux when $\phi_o > \phi_g$) and the corresponding bed height is smaller than for cylindrical and converging thickeners. Further, for diverging thickeners there should be no problem with buildup of particles on the walls. However it may prove difficult to remove the underflow from such thickeners. A possible remedy is to design a thickener that diverges over most of its length and then converges rapidly (truncated asymmetrical diamond shape). For any flux β (when $\phi_o > \phi_g$) and ϕ_u, the physical bed height H as a function of slope σ (which is a function of θ and R_0) can be determined from the above analysis. For a chosen value of the slope, the diverging part of the thickener should have the corresponding height H. Adjoin to this the converging section with internal angle θ larger than the angle of repose of the particles (so that particle buildup is avoided). In this end section ϕ will only increase slightly; hence the underflow will be a little larger than ϕ_u.

We have only obtained numerical results for thickeners with straight-sided walls, but the analysis applies to any shape. Therefore the following interesting optimization problem arises: Determine the thickener wall shape that leads to maximal throughput Q_p for a given underflow concentration ϕ_u and bed height H (when $\phi_o > \phi_g$), or alternatively, a maximal ϕ_u for given Q_p and H (in both modes of operation). Our proposition for a thickener design outlined above is an initial attempt at solving this general problem.

Notation

$a(Z)$ = scaled cross-sectional area of thickener, Eq. 69
a_p = characteristic particle dimension
A_0 = cross-sectional area of thickener at feed input point
$A(z)$ = cross-sectional area of thickener
$B(\Phi, \phi_u, \phi_o)$ = scaled drag function, Eq. 65
$f(\Phi)$ = scaled compressional yield stress, Eq. 64
$\bar{F}(z, t)$ = cross-sectional average of function $F(z, x, t)$, Eq. 24
F_h = hydrodynamic drag force per unit volume of suspension
g = gravitational acceleration
H = bed height in thickener
$K(\phi)$ = hydraulic conductivity of suspension, Eq. 6
L = scaled bed height, Eq. 68
$M(\Phi, Z)$ = effective weight function, Eq. A13
p = local network (particle) pressure
$P_y(\phi)$ = compressive yield stress of suspension
$P_{os}(\phi)$ = osmotic pressure of stable suspension
Q_p = total particle volumetric flow rate through thickener, Eq. 33
Q_w = total fluid volumetric flow rate through thickener at underflow point, Eq. 34

$r(\phi)$ = hindered settling factor, Eq. 1
$R(z)$ = radius of thickener
R_0 = radius at thickener feed input point
u_{St} = Stokes settling velocity of isolated particle, Eq. 2
v = local particle velocity
v_x = radial component of v
v_z = z component of v
V_p = average particle volume
w = local fluid velocity
w_x = radial component of w
w_z = z component of w
x = horizontal coordinate in thickener
Y = rescaled Z, Eq. 83
Y_c = scaled Z_c, Eq. 86
Y_0 = scaled z_0
Y^* = scaled z^*
z = vertical position coordinate in thickener
z_c = vertical position of top of consolidation zone
z_0 = negative of z coordinate of feed input point, Eq. 88
z^* = Eq. 59
Z = scaled z coordinate, Eq. 61
Z_c = scaled z_c, Eqs. 74, 75

Greek letters

$\alpha(Y)$ = scaled cross-sectional area of thickener, Eqs. 85, 89
β = scaled particle flux, Eq. 67
$\Delta\rho$ = density of solid minus density of suspending fluid
η = fluid viscosity
$\kappa(\phi)$ = dynamic compressibility, Eq. 13
λ_{St} = Stokes drag coefficient (6π for sphere)
$\Lambda(\Phi)$ = scaled inverse compressibility, Eq. 66
Λ_c = $\Lambda(\Phi_c)$
$\Pi(Z)$ = scaled network pressure, Eq. 63
$\phi(z)$ = particle volume fraction at position z
ϕ_{cp} = close packing volume fraction
ϕ_g = network gel point
ϕ_o = feed volume fraction of particles
ϕ_u = underflow volume fraction
ϕ_u^∞ = asymptote for ϕ_u
$\Phi(Z)$ = scaled volume fraction, Eq. 62
Φ_c = value of Φ at top of consolidation zone, Eqs. 74, 75
σ = measure of slope of thickener walls, Eq. 90
θ = angle thickener wall makes with interior horizontal of thickener, Eq. 87

Appendix

To reveal the nature of the boundary layer at the start of the consolidation zone, we proceed as follows. We define $\Phi^{(0)}(Z)$ to be the $\mathcal{O}(1)$ function that solves Eq. 81 and satisfies the boundary condition

$$\Phi^{(0)}(Z_c) = \Phi_c \tag{A1}$$

The solution $\Phi(Z)$ of the exact Eqs. 71–73 we write as

$$\Phi(Z) = \Phi^{(0)}(Z) + \Lambda_c \Phi^{(1)}\left(\frac{Z - Z_c}{\Lambda_c}\right) \tag{A2}$$

where

$$\Lambda_c = \Lambda(\Phi_c) \ll 1 \tag{A3}$$

Since

$$\Phi(Z_c) = \Phi_c \tag{A4}$$

we require

$$\Phi^{(1)}(0) = 0 \tag{A5}$$

As discussed above, the exact solution must satisfy

$$\left.\frac{d\Phi}{dZ}\right|_{Z_c} = 0 \tag{A6}$$

so that $\Phi^{(1)}$ must also satisfy

$$\Phi^{(1)\prime}(0) = -\left.\frac{d\Phi^{(0)}}{dZ}\right|_{Z_c} \tag{A7}$$

from Eq. A2. This is sufficient to establish that $\Phi^{(1)}$ is a $\mathcal{O}(1)$ function of its argument and that we have

$$\Lambda_c \Phi^{(1)}\left(\frac{Z - Z_c}{\Lambda_c}\right) \ll \Phi^{(0)}(Z) \tag{A8}$$

It follows that for any analytic function $G(\Phi, Z)$ we may write

$$G(\Phi, Z) = G(\Phi^{(0)}, Z) + \frac{\partial_G}{\partial\Phi}(\Phi^{(0)}, Z)\Lambda_c\Phi^{(1)} + \frac{1}{2}\frac{\partial^2 G}{\partial\Phi^2}(\Phi^{(0)}, Z)[\Lambda_c\Phi^{(1)}]^2 + \mathcal{O}(\Lambda_c^3) \tag{A9}$$

We define the excess pressure $\Pi^{(1)}(Z)$ by

$$\Pi(Z) = f[\Phi(Z)] + \Pi^{(1)}(Z) \tag{A10}$$

where, from the scaling argument above, we know $\Pi^{(1)}(Z)$ is $\mathcal{O}(\Lambda_c)$. It follows directly from the definition of Z_c that

$$\Pi^{(1)}(Z_c) = 0 \tag{A11}$$

Substituting Eq. A10 into Eq. 71, we obtain

$$\frac{d\Pi^{(1)}}{dZ} + \frac{df(\Phi)}{dZ} = LM(\Phi, Z) \tag{A12}$$

where, for convenience, we define

$$M(\Phi, Z) = \Phi\left[1 - \frac{\beta}{a(Z)}B(\Phi, \phi_u, \phi_o)\right] \tag{A13}$$

Using Eq. A9, we may rewrite Eq. A12 correct to $\mathcal{O}(\Lambda_c)$ as

$$\frac{d}{dZ}\left\{\Pi^{(1)} + \Lambda_c f'[\Phi^{(0)}]\Phi^{(1)} + \frac{\Lambda_c^2}{2}f''[\Phi^{(0)}][\Phi^{(1)}]^2\right\} = L\Lambda_c\frac{\partial M}{\partial\Phi}(\Phi^{(0)}, Z)\Phi^{(1)} + \mathcal{O}(\Lambda_c^2) \tag{A14}$$

where we have used the result

$$\frac{df[\Phi^{(0)}]}{dZ} = LM(\Phi^{(0)}, Z) \tag{A15}$$

which follows directly from the definition of $\Phi^{(0)}(Z)$. We have kept the $\mathcal{O}(\Lambda_c^2)$ term on the lefthand side of Eq. A14 since differentiating this term as required will produce an $\mathcal{O}(\Lambda_c)$ term.

Integrating Eq. 14, we obtain, to $\mathcal{O}(\Lambda_c^2)$

$$\Pi^{(1)}(Z) = -\Lambda_c f'[\Phi^{(0)}]\Phi^{(1)} - \frac{\Lambda_c^2}{2} f''[\Phi^{(0)}][\Phi^{(1)}]^2 + L\Lambda_c \int_{Z_c}^{Z} d\xi \frac{\partial M}{\partial \Phi}(\Phi^{(0)}(\xi), \xi)\Phi^{(1)}\left(\frac{\xi - Z_c}{\Lambda_c}\right) \quad \text{(A16)}$$

with the aid of Eqs. A5 and A11. To obtain $\Pi^{(1)}(Z)$ correct to $\mathcal{O}(\Lambda_c)$ we may neglect the second term on the righthand side since it is clearly $\mathcal{O}(\Lambda_c^2)$. The third term can also be neglected since it too is $\mathcal{O}(\Lambda_c^2)$, provided $\Phi^{(1)}$ is bounded as its argument tends to infinity. This is in fact the case as we demonstrate below. Thus we may write

$$\Pi^{(1)}(Z) = -\Lambda_c f'[\Phi^{(0)}(Z)]\Phi^{(1)}\left(\frac{Z - Z_c}{\Lambda_c}\right) + \mathcal{O}(\Lambda_c^2) \quad \text{(A17)}$$

Equation 73 can be written as

$$\frac{d\Phi}{dZ} = \frac{\Phi a(Z)}{\Lambda(\Phi)}\Pi^{(1)} \quad \text{(A18)}$$

which to leading order is

$$\frac{d\Phi^{(0)}}{dZ} + \Lambda_c \frac{d\Phi^{(1)}}{dZ}\left(\frac{Z - Z_c}{\Lambda_c}\right) = -\frac{\Phi^{(0)}\Lambda_c f'[\Phi^{(0)}]a(Z)}{\Lambda[\Phi^{(0)}]}\Phi^{(1)}\left(\frac{Z - Z_c}{\Lambda_c}\right) + \mathcal{O}(\Lambda_c) \quad \text{(A19)}$$

The change of variable

$$\zeta = \frac{Z - Z_c}{\Lambda_c} \quad \text{(A20)}$$

produces the differential equation

$$\frac{d\Phi^{(1)}}{d\zeta}(\zeta) + \frac{\Phi^{(0)}\Lambda_c f'[\Phi^{(0)}]a(Z)}{\Lambda[\Phi^{(0)}]}\Phi^{(1)}(\zeta) = -\frac{d\Phi^{(0)}}{dZ} \quad \text{(A21)}$$

where $\Phi^{(0)}$ and $a(Z)$ have argument $Z_c + \Lambda_c\zeta$. We see from Eq. A21 that $\Phi^{(1)}(\zeta)$ is varying on a length scale $\zeta \sim 1$. It follows that we may replace the argument of $\Phi^{(0)}$ and $a(Z)$ by Z_c to leading order in Λ_c in the differential equation for $\Phi^{(1)}(\zeta)$. We obtain therefore,

$$\frac{d\Phi^{(1)}}{d\zeta} + [\Phi_c f'(\Phi_c)a(Z_c)]\Phi^{(1)} = -\left.\frac{d\Phi^{(0)}}{dZ}\right|_{Z_c} + \mathcal{O}(\Lambda_c) \quad \text{(A22)}$$

with solution

$$\Phi^{(1)}(\zeta) = -\frac{\left.\frac{d\Phi^{(0)}}{dZ}\right|_{Z_c}}{\Phi_c f'(\Phi_c)a(Z_c)}[1 - e^{-\Phi_c f'(\Phi_c)a(Z_c)\zeta}] \quad \text{(A23)}$$

We observe that $\Phi^{(1)}(\zeta)$ is bounded as $\zeta \to \infty$, as required above. Substituting Eqs. A17 and A2 into Eq. A10 we obtain

$$\Pi(Z) = f[\Phi^{(0)}(Z)] + \mathcal{O}(\Lambda_c^2) \quad \text{(A24)}$$

which is a stronger result than our scaling argument result, Eq. 76. We note that the above argument has implicitly assumed that $f'(\Phi_c)$ is nonzero. This may not be the case in the $\phi_o < \phi_g$ mode of thickener operation (where Φ_c is ϕ_g/ϕ_u) when $P_y(\phi)$ has the form of Eq. 9 with $m > 1$. In this situation, the boundary layer analysis would need to be carried out at a sufficiently high order in Λ_c so that a nonvanishing leading order term in the differential equation for $\Phi^{(1)}(\zeta)$ could be obtained. This complication need not be examined further since the overall nature of the boundary layer is unaltered.

Literature Cited

Batchelor, G. K., "Sedimentation in a Dilute Suspension of Spheres," *J. Fluid Mech.*, **52,** 245 (1972).

Brown, W. D., "The Structure and Properties of Flocculated Colloids," Ph.D. Thesis, Univ. Cambridge (1987).

Buscall, R., J. W. Goodwin, R. H. Ottewill, and Th. F. Tadros, "The Settling of Particles through Newtonian and Non-Newtonian Media," *J. Colloid Interf. Sci.*, **85,** 78 (1982).

Buscall, R., I. J. McGowan, P. D. A. Mills, R. F. Stewart, D. Sutton, L. R. White, and G. E. Yates, "The Rheology of Strongly Flocculated Suspensions," *J. Non-Newtonian Fluid Mech.*, (1987).

Buscall, R., and L. R. White, "On the Consolidation of Concentrated Suspensions. I: The Theory of Sedimentation," *J. Chem. Soc. Faraday I,* **83,** 873 (1987).

De Guingand, N. J., "The Behaviour of Flocculated Suspensions in Compression," M. E. Thesis, Univ. Melbourne (1986).

Dixon, D. C., "Momentum-Balance Aspects of Free-Settling Theory. III: Transient Compression Resistance," *Separ. Sci. Technol.*, **13,** 753 (1978).

———, "Effect of Sludge Funneling in Gravity Thickeners," *AIChE J.*, **26,** 471 (1980).

Kops-Werkhoven, M. M., and H. M. Fijnant, "Dynamic Behavior of Silica Dispersions Studied near the Optimal Matching Point," *J. Chem. Phys.*, **77,** 2242 (1982).

Tiller, F. M., and Z. Khatib, "The Theory of Sediment Volumes of Compressible, Particulate Structures," *J. Colloid Interf. Sci.*, **100,** 55 (1984).

Tiller, F. M., and W. F. Leu, "Basic Data Fitting in Filtration," *J. Chinese Inst. Chem. Eng.*, **11,** 61 (1980).

Manuscript received Mar. 16 and May 4, 1987 in two parts, revision received Aug. 6, 1987.